PERGAMON

International Journal of Solids and Structures 38 (2001) 2233–2248

INTERNATIONAL JOURNAL OF SOLIDS and STRUCTURES

www.elsevier.com/locate/ijsolstr

Dynamics and stability of milling process

M.X. Zhao, B. Balachandran *

Department of Mechanical Engineering, University of Maryland, College Park, MD 20742, USA

Received 4 August 1999; in revised form 29 December 1999

Abstract

Numerical and experimental investigations conducted into the dynamics and stability of a range of milling operations are presented in this article. A unified mechanics based model developed to study workpiece–tool system dynamics is used for the numerical studies. This model, which allows for both regenerative effects and loss of contact effects, can be used for studying partial-immersion, high-immersion, and slotting operations. Loss of stability of periodic motions associated with milling operations is assessed by using Poincaré sections, and the numerical predictions of stable and unstable motions are found to compare well with corresponding experimental data. Bifurcations experienced by the periodic motions with respect to parameters such as axial depth of cut are numerically examined and discussed. The sensitivity of dynamics to tooth passing period, feed rate, and feed direction is also discussed. © 2001 Elsevier Science Ltd. All rights reserved.

Keywords: Dynamics; Stability; Milling process

1. Introduction

During certain cutting conditions, the motions of the workpiece–tool system are characterized by large amplitudes, which are not desirable for obtaining a good surface finish. The undesirable motions, which are often referred to as *chatter*, can result in wavy surfaces on the workpiece, inaccurate dimensions, and excessive tool wear. Following the initial efforts of Arnold (1946), an extensive number of efforts have been devoted to understanding chatter produced by regenerative mechanisms (e.g. Merritt, 1965; Tobias and Fishwick, 1958; Tobias, 1965; Tlusty, 1985). Tlusty and Polacek (1963) examined the possibility of chatter due to nonregenerative mechanisms such as mode coupling. Another nonregenerative mechanism that may lead to chatter is associated with nonlinearities due to intermittent engagement between a tool and a workpiece. This was numerically studied by Tlusty and Ismail (1981). In a related study, Balachandran et al. (1997) examined the influence of loss of contact type nonlinearities on the dynamics of an elastic structure subjected to aharmonic excitations. Davies and Balachandran (1999) examined the importance of modeling loss of contact type nonlinearities during partial-immersion milling operations through experiments and numerical simulations.

* Corresponding author. Tel.: +1-301-405-5309; fax: +1-301-314-9477.
E-mail address: balab@eng.umd.edu (B. Balachandran).

0020-7683/01/$ - see front matter © 2001 Elsevier Science Ltd. All rights reserved.
PII: S0020-7683(00)00164-5

A common approach, which is used to avoid chatter or move away from a region of chatter, is to change the parameters such as the axial depth of cut and the spindle speed. In order to choose parameters to ensure stable milling operations, a thorough understanding of the process dynamics for a range of milling operations is necessary. Related efforts in this regard include the studies of Sridhar et al. (1968), Tlusty (1985), Minis and Yanushevsky (1992), Altintas and Budak (1995), and Altintas and Lee (1996). By and large, in these efforts, predictions of instabilities have been made for full-immersion and high-immersion milling operations during which regenerative effects are likely to be dominant. As the immersion ratio is decreased, loss of contact effects due to intermittent cutting action associated with each cutter flute become important. There may also be a range of milling operations for which both regenerative effects and loss of contact effects can be important for prediction of instabilities. The consideration of only the regenerative effects in the studies of Sridhar et al. (1968), Minis and Yanushevsky (1992), and Altintas and Budak (1995) has enabled the use of tools available for stability analysis of linear systems with time periodic and time delay terms. However, the consideration of loss of contact effects as in the studies of Balachandran and Zhao (1999a,b) requires different stability considerations.

With the aim of developing a model for studying a range of milling operations, Balachandran and Zhao (1999a,b) developed a unified mechanics based model with features such as partial engagement of a tool with a workpiece, regenerative and loss of contact effects, tool flexibility, and workpiece flexibility. In the article of Balachandran and Zhao (1999a), results from the unified mechanics based model were compared with earlier results available in the literature and the importance of considering helical angle effects was pointed out. Balachandran and Zhao (1999b) presented a detailed description of the unified mechanics based model and provided preliminary results on dynamics and stability of milling operations obtained by using this model. The present article is a companion article to our earlier one, in which the focus is on model development. The focus of the current article is on dynamics and stability of milling operations. Stability charts and bifurcation diagrams for various milling operations are provided here along with a discussion on the sensitivity of the system dynamics to parameters such as immersion ratio and feed rate. The rest of this article is organized as follows. In Section 2, some features of the current model are outlined, and the results obtained by using this model are presented in the next section and compared with the corresponding experimental data. For completeness, Appendix A is provided to include some model details.

2. Unified mechanics based model

In this section, some aspects of the unified mechanics model are discussed. (A full discussion on the model is provided in the articles of Balachandran and Zhao (1999a,b)). In Fig. 1 shown below, a multi-degree-of-freedom model for the workpiece–tool system is illustrated along with a cylindrical end mill. The feed direction and spindle rotation are shown for an up milling operation. The cutter has a diameter $2R$, N number of flutes, and a helix angle η. The X-direction is oriented along the feed direction of the cutter and the feed rate is specified by f. The vertical axis of the tool is oriented along the Z-direction. Since the primary interest is in capturing the dynamic effects in the horizontal plane, and since the resonance frequencies associated with torsional modes and Z-direction vibration modes are expected to be higher than those associated with the other modes, they are not included in the current model.

The system differential equations are of the form

$$\begin{aligned} m_x\ddot{q}_x + c_x\dot{q}_x + k_x q_x &= F_x(t;\tau_1,\tau_2),\\ m_y\ddot{q}_y + c_y\dot{q}_y + k_y q_y &= F_y(t;\tau_1,\tau_2),\\ m_u\ddot{q}_u + c_u\dot{q}_u + k_u q_u &= F_u(t;\tau_1,\tau_2),\\ m_v\ddot{q}_v + c_v\dot{q}_v + k_v q_v &= F_v(t;\tau_1,\tau_2), \end{aligned} \tag{1}$$

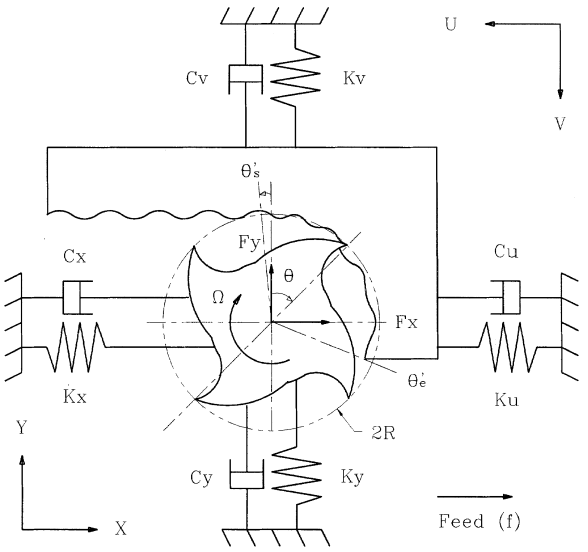

Fig. 1. Workpiece–tool system model.

where t represents time, an overdot indicates differentiation with respect to time, the variables q_x and q_y are used to describe tool motions, and the variables q_u and q_v are used to describe workpiece motions. Further, m_x and m_y are mass components for the tool, k_x and k_y are the stiffness components for the tool, c_x and c_y are the damping components for the tool, and F_x and F_y are forces acting on the milling tool. For the workpiece, m_u and m_v are mass components, k_u and k_v are stiffness components, c_u and c_v are damping components, and F_u and F_v are forces acting on the workpiece due to the cutting action. Other parameters in the figure that have not explicitly appeared in the system equations are the angular position of cutting tooth θ, the starting cutting angle θ_s, the exit angle θ_e, the tangential cutting force F_t, and the radial cutting force F_r.

The cutting forces are functions of machining parameters, such as immersion ratio and feed rate, and system dynamics. To calculate the cutting forces, the whole milling cutter is divided into a stack of infinitesimal disk elements along Z-axis. For each disk element, a refined orthogonal cutting method is applied to obtain the cutting force components. (As this method is not discussed in Balachandran and Zhao (1999b), a description of refined orthogonal cutting method is included for completeness in Appendix A.) The total cutting forces are then summed, through a spatial integration scheme, over all elements. The two spatial integration limits are functions of the workpiece–tool system dynamics, as discussed by Balachandran and Zhao (1999b). Numerical simulations are carried out by using the system of Eqs. (1) and the stability of motions associated with different milling operations are studied. For a stable cutting operation, the system motion will be a periodic motion with the basic frequency determined by the spindle rotation speed. Loss of stability of this periodic motion is assessed by using Poincarè sections in the numerical simulations (e.g., Nayfeh and Balachandran, 1995).

3. Results and discussion

In this section, results obtained in numerical and experimental investigations into the dynamics and stability of various milling operations are presented. The experiments were conducted on a high-speed machining testbed in the Manufacturing Engineering Laboratory of the National Institute of Standards

Table 1
Modal parameters of the tool

	Frequency (Hz)	Damping (%)	Stiffness (N/m)	Mass (Kg)
X	900.03	1.39	8.79×10^5	2.75×10^{-2}
Y	911.65	1.38	9.71×10^5	2.96×10^{-2}

and Technology (NIST). The cutter has a 30° helix angle and a diameter of 12.7 mm. The tool modal parameters, which were determined from transfer functions, are shown in Table 1. The workpiece is a rigid aluminum block whose specific cutting energy is chosen to be 6.0×10^8 N/m^2 and the proportionality factor is taken to be 0.3. For all the studies, the feed rate is fixed at 0.102 mm/tooth unless otherwise stated.

3.1. Stability charts for various immersions

For the corresponding simulations, the cutter is modeled as having a flat end. In Fig. 2, stability charts are provided in the space of axial depth of cut (ADOC) and spindle speed for milling operations ranging from full-immersion (slotting) to partial (10%) immersion cuts. (When the radial depth of cut (RDOC) is equal to the cutter diameter, there is 100% immersion or full-immersion of the tool in the workpiece.) As noted earlier, the loss of stability of a periodic motion is assessed by using a Poincaré section (e.g. Nayfeh and Balachandran, 1995). To construct the stability charts, the stability limits are obtained by gradually increasing the axial depth of cut while holding all of the other parameters constant until an instability is detected. This procedure is repeated at different spindle speeds to construct the stability diagram. In the different charts, the typical bifurcation associated with a loss of stability of a periodic motion is a Neimark bifurcation. The exceptions where period-doubling bifurcations are believed to occur are marked by diamond shaped markings.

For full-immersion operations, typical lobe-shape patterns that can be predicted on the basis of regenerative effects alone are observed. The loss of stability in all cases are found to be due to Neimark

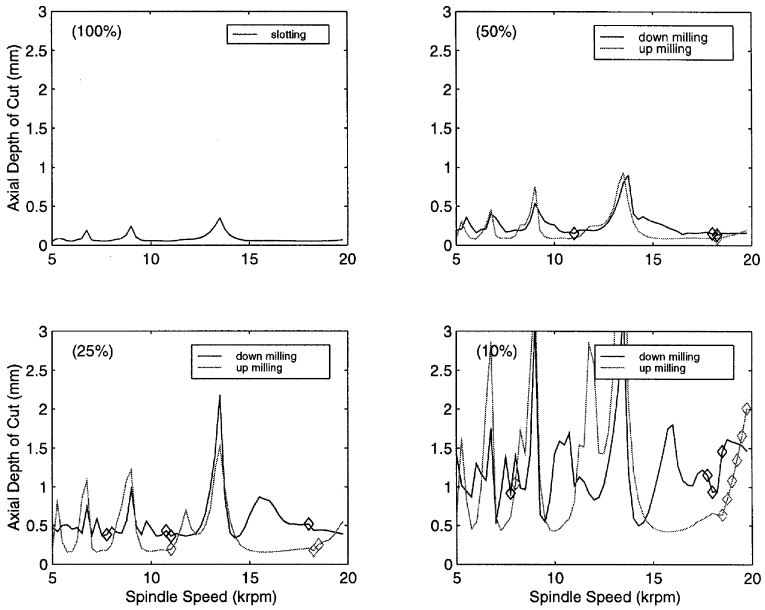

Fig. 2. Stability charts for 100%, 50%, 25%, and 10% immersion milling operations.

bifurcations of periodic motions. But as the immersion ratio is reduced, distortions from the lobe structure seen for the full-immersion case are noticeable. In addition, the charts for the up milling and down milling cases are different from one another. These differences are believed to be due to the loss of contact effects that become prominent as the immersion ratio is reduced. In some cases, it appears that the lobes undergo splitting. Also, period-doubling bifurcations are found in addition to Neimark bifurcations. The post-bifurcation motions may be associated with chatter.

3.2. Comparisons with experimental results and bifurcation diagrams

As discussed in the context of Fig. 2, stability charts of partial-immersion milling operations can be determined by both regenerative effects as well as loss of contact effects, and hence, the charts can be qualitatively and quantitatively different from those predicted on the basis of linear, time periodic systems with time delays. Experiments were conducted to verify the stability predictions made for a 25% immersion down milling operation. In order to account for the round nose of the cutter used in the experiments, the specific cutting energy of aluminum is chosen to be 2.939×10^8 N/m^2 in the corresponding simulations. The stability predictions obtained through time domain simulations are compared with experimental results in Fig. 3. In addition, stability predictions based on a previous model, which includes only regenerative effects, are also provided. It is seen that the stability predictions based on the model, which includes both regenerative and loss of contact effects, are in good agreement with the experimental results. In particular, at high spindle speeds, stability predictions based on a model that includes only regenerative effects differ considerably from experimental observations. However, numerical results based on simulations, which account for both regeneration and loss of contact effects, are in good agreement with the experiments.

For 25% immersion down milling operations, the numerically constructed bifurcation diagrams obtained at spindle speeds of 20,000 and 11,000 rpm are shown in the first and second columns of Fig. 4, respectively. The diagrams obtained for the forward and reverse sweeps of the control parameter ADOC in each case are shown. The occurrence of a Neimark bifurcation at an ADOC of about 0.9 mm is suggested by the results

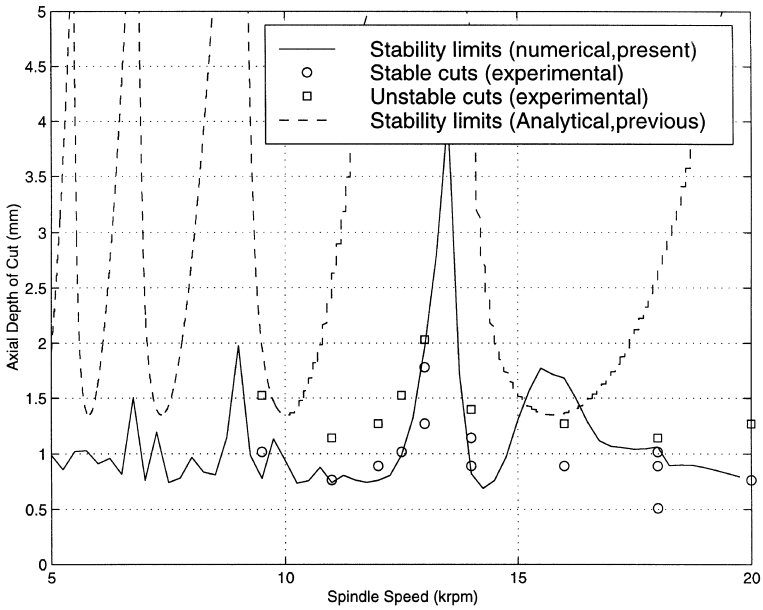

Fig. 3. Stability predictions for 25% immersion down milling operation.

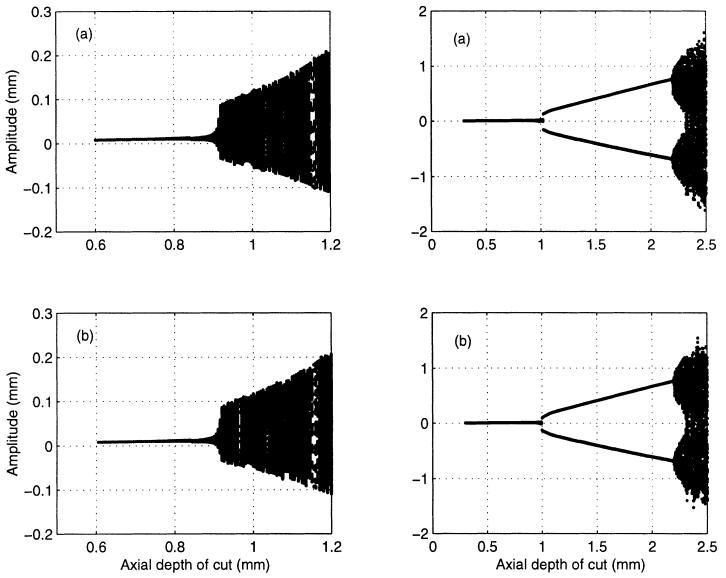

Fig. 4. Bifurcation diagrams on Poincaré sections for 20,000 rpm case in the first column and 11,000 rpm case in the second column: (a) forward sweep of ADOC and (b) backward sweep of ADOC.

shown for the 20,000 rpm case, and the occurrence of a period-doubling bifurcation at an ADOC of about 1.0 mm is suggested by the results shown for the 11,000 rpm case. The characteristics of the post-bifurcation motions are different in the two cases.

In Fig. 5, time histories, projections of state-space plots, power spectra, and Poincaré sections associated with pre-bifurcation and post-bifurcation motions at a spindle speed of 20,000 rpm are shown. In the last row, the corresponding experimental results are included. The pre-bifurcation motion, which corresponds to a ADOC of 0.76 mm, is a stable periodic motion. The post-bifurcation motion, which corresponds to a ADOC of 1.20 mm, is a stable two-period quasiperiodic motion. This motion follows a Neimark bifurcation, which is responsible for the introduction of the incommensurate frequency f_c that is close to the tool natural frequency. Stable and unstable cuts are associated with the pre-bifurcation and post-bifurcation motions, respectively. There is also a good agreement between the simulation results and the experimental results. In Fig. 6, features associated with pre-bifurcation and post-bifurcation motions at a spindle speed of 11,000 rpm are shown. A period-doubling bifurcation introduces a subharmonic of the basic frequency in the post-bifurcation motion. In Fig. 7, numerical results are presented to illustrate the occurrence of a subcritical Neimark bifurcation at a spindle speed of 5000 rpm. The occurrence of subcritical bifurcations are important to note because typically, when one encounters chatter in an experimental situation, a tendency is to reduce the ADOC. This reduction needs to be sufficient to take one out of the subcritical region for realizing stable cutting.

3.3. Tooth contact time variation

As discussed by Balachandran and Zhao (1999b), a common assumption made in milling models is that the tooth contact time is constant and does not change from one spindle cycle to the next. The numerical results presented in Fig. 8 show how the tooth contact time for a single tooth changes from one spindle cycle to another during long-time motions for a spindle speed of 20,000 rpm. The ADOC is used as a control parameter and it is varied in a quasi-static manner to generate the results shown in the figure. The

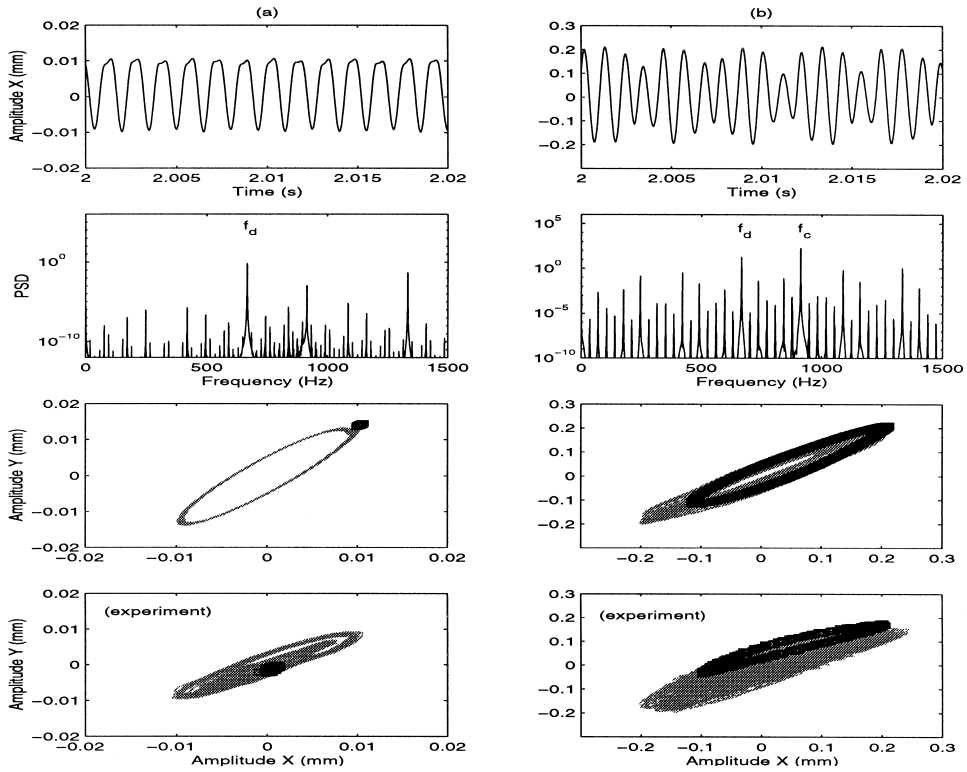

Fig. 5. Pre-bifurcation and post-bifurcation motions at 20,000 rpm: (a) ADOC = 0.76 mm (stable cut) and (b) ADOC = 1.20 mm (unstable cut).

contact time determined over each cycle of about 50 cycles of long-time motions is shown at each value of ADOC. The graph can be divided into three regions. For ADOC less than 0.75 mm, the contact time increases monotonically with respect to ADOC but remains constant from one spindle cycle to next at each ADOC. The associated motions, which are periodic at the tooth cutting frequency, are characterized by "small" amplitude motions. The near linear variation in the contact time can be attributed to the tool helix angle. For ADOC larger than 0.9 mm, there is a scatter in the tooth contact time variation at each ADOC. In these regions, unstable cuts are associated with the system motions. The region corresponding to a ADOC larger than 0.75 mm and less than 0.9 mm is a critical region because the loss of stability of periodic motion leading to chatter occurs at the end of this region. It is quite clear from the graph that even prior to the Neimark bifurcation point at an ADOC of about 0.9 mm, there is a considerable variation in the tooth contact time from one spindle cycle to the next cycle of the stable motions. So, models assuming a constant contact time are likely to lead to erroneous results in predictions of instabilities. Here, it is believed that the partial tooth engagement feature described by Balachandran and Zhao (1999b) is important for capturing the tooth contact time variation accurately.

3.4. Effect of number of previous tooth pass periods on stability

When more than one tooth cutting action is involved in the formation of the workpiece surface, an appropriate number of previous tooth passing periods needs to be considered to fully account for the multiple regeneration effects. In some cases, the dynamic uncut chip thickness, which is described by

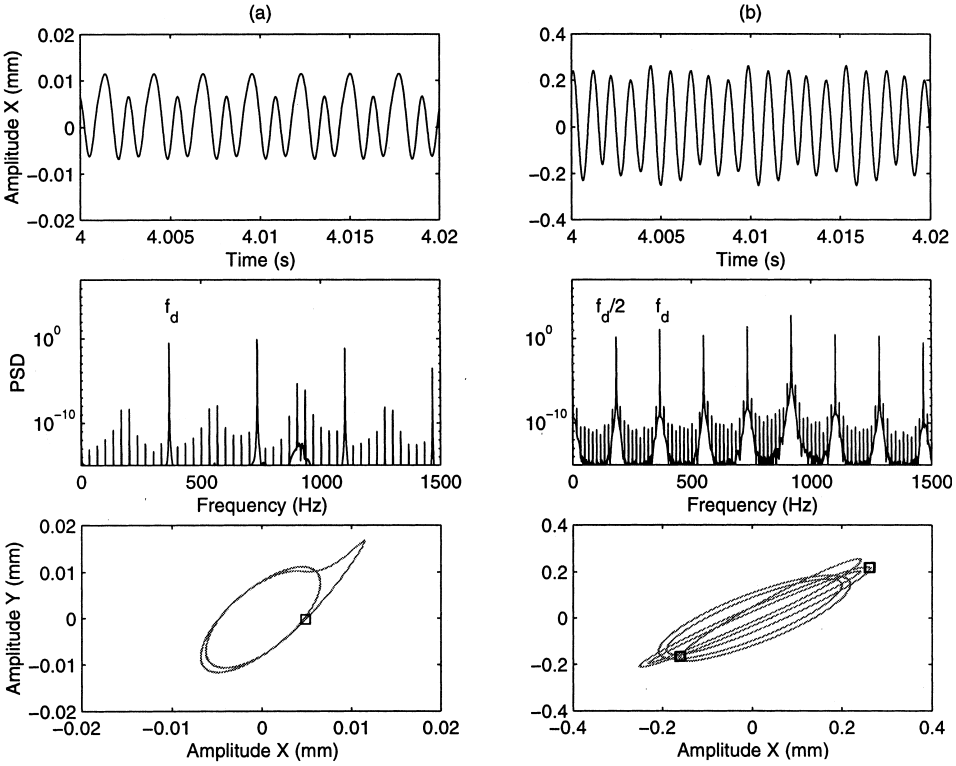

Fig. 6. Pre-bifurcation and post-bifurcation motions at 11,000 rpm: (a) ADOC = 0.60 mm (stable cut) and (b) ADOC = 1.14 mm (unstable cut).

Eq. (A.3) in Appendix A, may need to be determined by considering at least two or more previous tooth cutting actions. This means that the index j in Eq. (A.4) needs to have an integer value larger than or equal to two. The importance of considering the appropriate number of previous tooth pass periods for the stability of partial-immersion operations is illustrated by the results presented in Fig. 9.

Here, for 25% immersion down milling operations, a series of stability charts generated by considering different values of the index j are presented. When only the immediate previous tooth cutting action is considered, the stability chart appears to be smooth with high peaks. As the number of previous tooth pass periods is increased, the stability chart starts differing considerably from that obtained with one tooth pass period. The peaks at the intersection of two lobes are lower than those previously obtained. It is expected that as the number of previous tooth pass periods is increased, the regenerative effects can become stronger, and as a consequence, result in lower stability limits. As the index j is increased to three and then to four, the corresponding stability charts are close to each other. The results shown in Fig. 9 are illustrative of the importance of considering a sufficient number of previous tooth pass periods in determining stability boundaries.

3.5. Effect of feed rate on stability

The feed rate is represented by the parameter f in Eq. (A.4) and the subsequent equations in Appendix A. As shown there, the dynamic uncut chip thickness depends on the feed rate. In other studies, in which full-immersion and high-immersion operations are only considered, the feed rate does not affect the stability

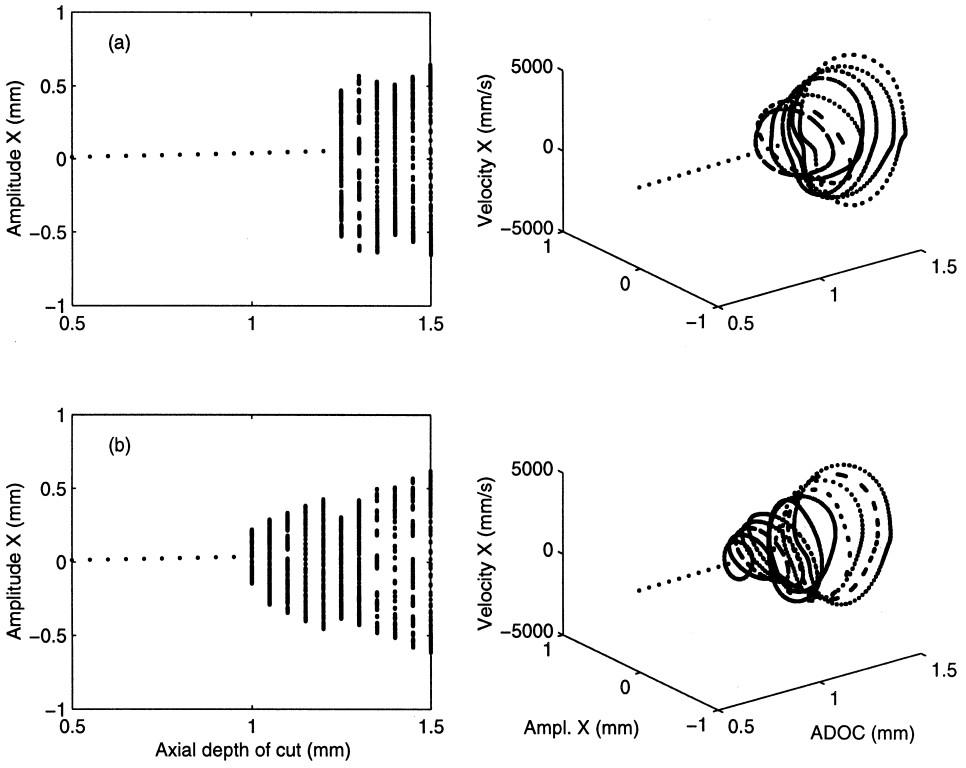

Fig. 7. Sub-critical Neimark bifurcation at 5,000 rpm: (a) forward sweep of ADOC and (b) backward sweep of ADOC.

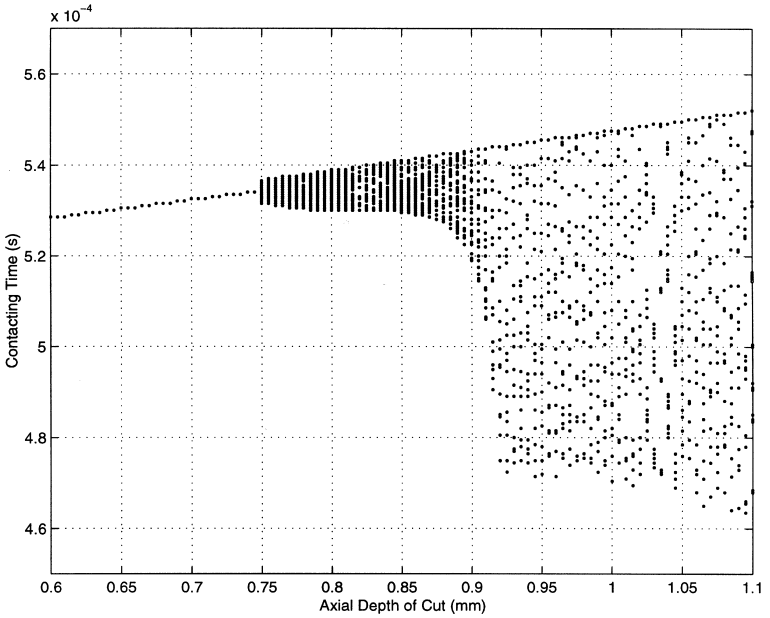

Fig. 8. Tooth contact time versus ADOC.

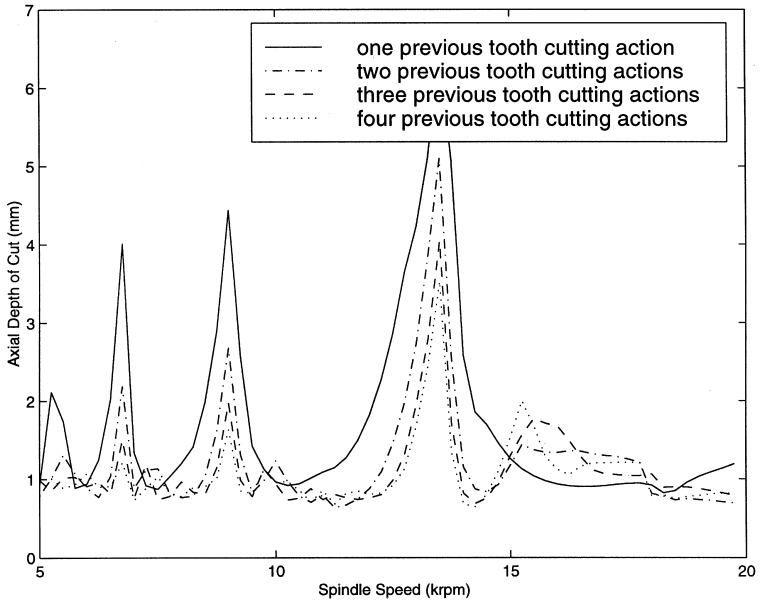

Fig. 9. Stability charts: effect of number of previous tooth pass periods.

predictions obtained on the basis of linear, time periodic systems with time delays. However, as shown next, the feed rate can be quite important in predicting the stability boundaries for partial-immersion operations where loss of contact effects can be quite significant.

In Figs. 10 and 11, the effect of feed rate on the stability charts of a full-immersion operation and a 25% immersion operation are shown, respectively. The nominal feed rate that has been used throughout for the previous simulations and during the experiments is $f = 0.102$ mm/tooth. Apart from this rate, two other feed rates are considered. One of them is higher with a value of $f = 0.510$ mm/tooth, and the other rate is lower with a value of $f = 0.0204$ mm/tooth. For full-immersion milling operations, the effect of feed rate on stability limits is not pronounced. However, for the 25% immersion milling operation, the stability limits for the nominal and lower feed rates remain close while the stability limits for the higher feed rate differ considerably from those obtained at the nominal feed rate. This is attributed to the loss of contact effects, which can be dominant during partial-immersion operations.

3.6. Effect of feed direction on stability

When a flexible tool is used in milling operations, motions along the two orthogonal directions in the horizontal plane can force the tool tip to move along an elliptical orbit and the associated characteristics will depend upon the relative participation of the respective modal components along the two orthogonal directions. Depending upon the modal parameters associated with the two directions, instability due to mode coupling (equivalent to flutter instability) may occur as discussed by Tlusty and Ismail (1981). Here, the influence of the tool modal parameters on the stability charts for partial-immersion operations is investigated.

In Fig. 12, several stability charts for 25% immersion milling operations are presented. The curves marked with the legend "original" refers to the same system configuration as used in the previous cases, and the curves marked with the legend "reversed" refers to a system where the two sets of modal parameters along X- and Y-directions in the original system have been switched. In a machining context, this is

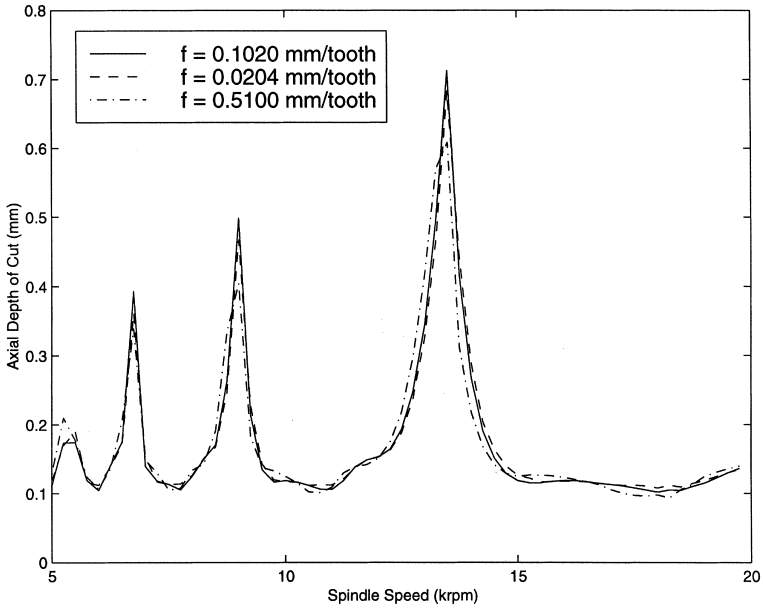

Fig. 10. Stability charts for a 100% immersion operation: effect of feed rate.

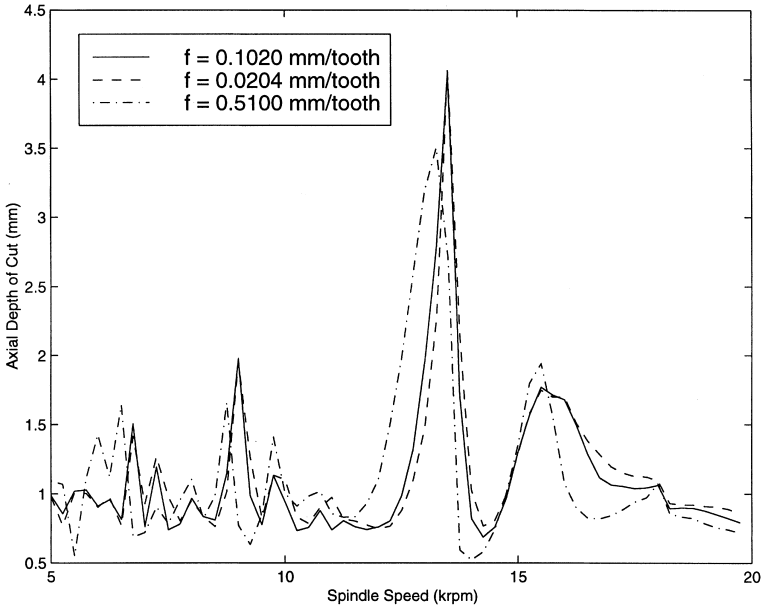

Fig. 11. Stability charts for 25% immersion operation: effect of feed rate.

equivalent to having the feed direction of the original system rotated by an angle of 90°. Results for both down milling and up milling operations are included. For the case considered, the stability limits of the original system are much higher than the corresponding stability limits obtained in the reversed system during the down milling operation. The situation is the opposite when the up milling operation is

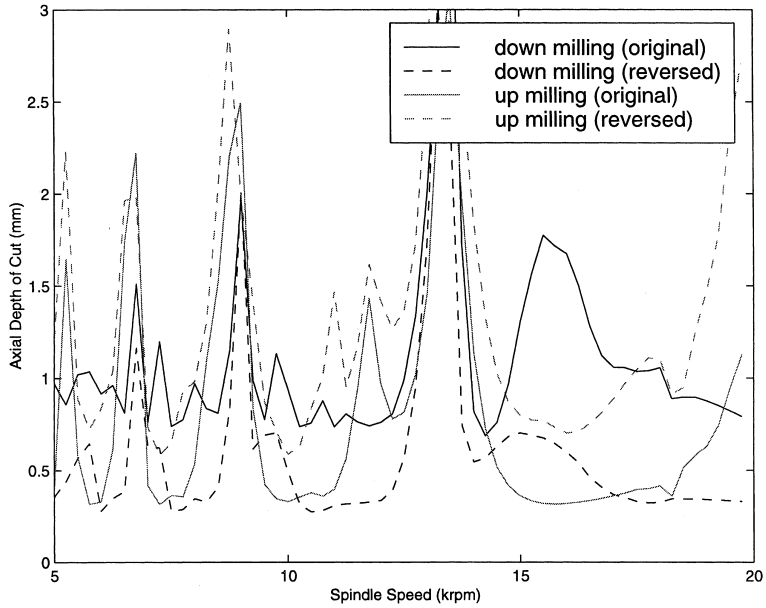

Fig. 12. Stability limits for different tool orientations.

considered. Hence, a good knowledge of the workpiece–tool system dynamics and stability can help one choose an appropriate feed direction for higher machining stability. This can be important for path planning in machining operations.

4. Closure

A unified mechanics based model has been used to simulate the dynamics of a workpiece–tool system for a range of milling operations. Both regenerative effects and loss of contact effects are taken into account and their effect on the stability is investigated. From the results obtained thus far, it can be stated that stability predictions based on linear, time periodic systems with time delays may be sufficient for full-immersion and high-immersion milling operations. However, this is not true of partial-immersion milling operations, for which loss of contact effects have a strong influence on the stability boundaries. The different instabilities that arise during partial-immersion operations have been addressed, and changes in stability charts with respect to aspects such as immersion ratio, feed rate, number of previous tooth pass periods, and feed direction have also been examined. The numerical results obtained are also found to compare well with corresponding experimental results. It has also been pointed out that the common assumption made in current milling models that the tooth contact time is constant from one spindle cycle to the next may not be true for all milling operations, in particular, for partial-immersion operations.

Acknowledgements

Support received for this work from the US Department of Commerce, National Institute of Standards and Technology through grant no. 60NANB6D0052 is gratefully acknowledged. Dr. Chris Evans is the

technical monitor for this contract. Dr. M.A. Davies and Dr. J.R. Pratt of NIST are thanked for the experimental results and related discussions and interactions.

Appendix A

For completeness, some details of the mechanics based model discussed by Balachandran and Zhao (1999b) are included here along with other details not discussed in that article. First, some of the details associated with the determination of the cutting forces are discussed. If the helical tool is decomposed into a set of infinitesimal disk elements along its axis, the cutting action at the interface of an element and the workpiece can be explained as an oblique cutting process, which is illustrated in Fig. 13. Here, η is the inclination angle (with $\eta = 0$ for orthogonal cutting), φ_n is the normal rake angle, and η_c is the chip flow angle. Based on experimental observations that the chip flow angle is close to the inclination angle in oblique cutting, the cutting action in the normal cutting plane can be approximated as orthogonal cutting because the chip flow can be considered to be two dimensional (Lin and Oxley, 1972).

In Fig. 14, the decomposition of the cutting velocity vector into two components on the workpiece surface is shown. Component V_1 is within the normal cutting plane, and component V_2 is along the perpendicular direction to this plane. Due to component V_2, there is a relative (rigid body) sliding motion between the rake face of the tool and the inner surface of the chip (Fig. 13).

The oblique cutting action can be modeled as having the following two force components: (a) orthogonal cutting along the direction of V_1 that generates the forces F_c and F_n and (b) a relative sliding motion between the tool and the chip along the direction of V_2 that generates a frictional force F_μ as shown in Fig. 13. F_c is the thrust force and F_n is the normal force that are associated with orthogonal cutting process within the normal cutting plane, which can be determined by using orthogonal cutting theory from the machining

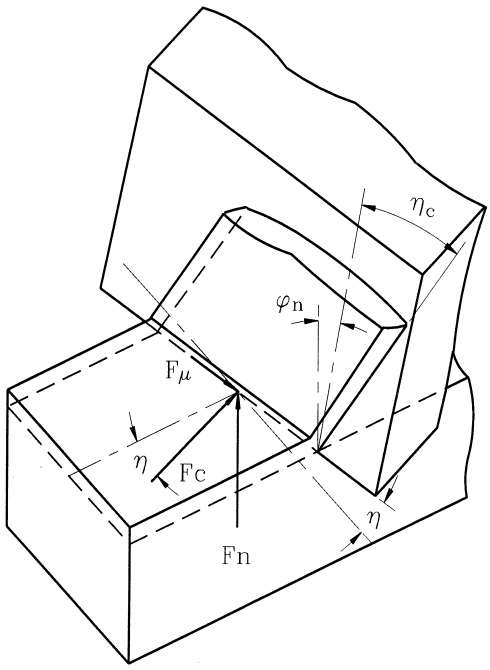

Fig. 13. Oblique machining: cutting force components are shown along n, c, and μ directions.

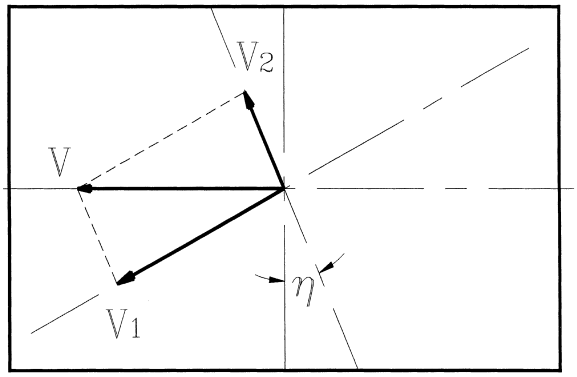

Fig. 14. Decomposition of the cutting velocity vector.

parameters (Oxley, 1989). In simple linear orthogonal cutting model, the two components of the cutting forces can be finally reduced to be proportional to the product of the width of cut w and uncut chip thickness h. Including the scaling effect of inclination angle η, they can be expressed as

$$\begin{aligned} F_c &= \frac{k_t h w}{\cos \eta}, \\ F_n &= k_n F_c, \end{aligned} \tag{A.1}$$

where k_t is the specific cutting energy and k_n is proportionality factor associated with orthogonal cutting. Having obtained F_c and F_n, one can determine the frictional force F_μ from Fig. 15 as being proportional to the pressure force P:

$$F_\mu = \mu P = \mu[F_c \cos \varphi_n - F_n \sin \varphi_n], \tag{A.2}$$

where μ is the dynamic friction coefficient for the sliding motion between the inner surface of the chip and the rake face of the tool.

In the above approach, which is named as "refined orthogonal cutting method", the cutting forces in oblique machining are approximated in terms of orthogonal cutting parameters. The forces determined in the static case above are extended to the dynamic case by replacing the static chip thickness h in Eq. (A.1) with the dynamic uncut chip thickness. This thickness is given by

$$h(t,i,z) = A(t) \sin \theta(t,i,z) + B(t) \cos \theta(t,i,z), \tag{A.3}$$

where i refers to a cutting tooth, z refers to the axial location along the tooth, and $A(t)$ and $B(t)$ represent the respective relative motions of workpiece–tool system along the X- and Y-directions; $\theta(t,i,z)$ represents the position angle; then, including previous tooth cutting actions, one can write these motions in the form

$$\begin{aligned} A(t) &= q_x(t) - q_x(t - j\tau_1) + q_u(t) - q_u(t - j\tau_1) + jf\tau_1, \\ B(t) &= q_y(t) - q_y(t - j\tau_2) + q_v(t) - q_v(t - j\tau_2), \end{aligned} \tag{A.4}$$

where τ_1 and τ_2 are the respective one tooth cutting periods along X and Y directions, and j is the number of a previous tooth cutting action associated with maximum relative displacement between the tool and workpiece along their positive radial directions in which the tool and workpiece move toward each other. The time delay terms τ_1 and τ_2 can be calculated from the following two equations:

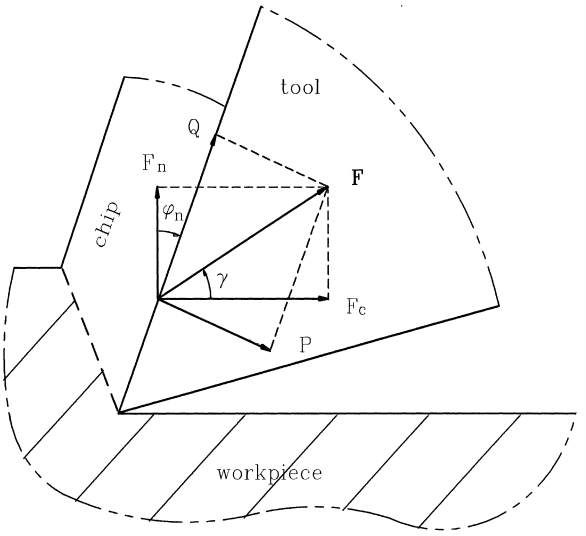

Fig. 15. Cross-section along normal cutting plane.

$$\tau_1 = \frac{1}{\Omega N}, \qquad \tau_2 = \frac{4\pi R\Omega}{4\pi R\Omega + f}\tau_1, \tag{A.5}$$

In Eq. (A.5), Ω is the spindle rotation speed and f is the feed rate. The difference between τ_1 and τ_2, which is due to the feed motion, is usually less than 2%. In the simulations, the delay terms as well as the value of j are determined by the following relations for limited numbers of the considered delay terms

$$\begin{aligned} q_x(t-j\tau_1) - jf\tau_1 + q_u(t-j\tau_1) &= \max\{q_x(t-\tau_1) - f\tau_1 + q_u(t-\tau_1), \\ &\quad q_x(t-2\tau_1) - 2f\tau_1 + q_u(t-2\tau_1), \ldots\}, \\ q_y(t-j\tau_2) + q_v(t-j\tau_2) &= \max\{q_y(t-\tau_2) + q_v(t-\tau_2), q_y(t-2\tau_2) + q_v(t-2\tau_2), \ldots\} \end{aligned} \tag{A.6}$$

The maximum allowable limit for j and the values of τ_1 and τ_2 can affect the regeneration during the simulation of the cutting process. Other details about the mechanics model can be found in the article of Balachandran and Zhao (1999b).

References

Altintas, Y., Budak, E., 1995. Analytical prediction of stability lobes in milling. Annals of the CIRP 44 (1), 357–362.

Altintas, Y., Lee, P., 1996. A general mechanics and dynamics model for helical end mills. Annals of CIRP 45, 59–64.

Arnold, R.N., 1946. The mechanism of tool vibration in the cutting of steel. In: Proceedings of the Institute of Mechanical Engineers, p. 154.

Balachandran, B., Zhao, M.X., Li, Y.Y., 1997. Dynamics of elastic structures subjected to impact excitations. In: Moon, F. (Ed.), Applications of Nonlinear and Chaotic Dynamics in Mechanics. Kluwer Academic Publishers, The Netherlands.

Balachandran, B., Zhao, M.X., 1999a. Dynamics and stability of milling process. In: Weber, H.I., Goncalves, P.B., Jasuik, I., Pamplona, D., Steele, C., Bevilacqua, L. (Eds.), IT Applied Mechanics in the Americas: Dynamics, vol. 8. American Academy of Mechanics, Philadelphia, USA and Brazilian Society of Mechanical Sciences, Rio de Janeiro, Brazil, pp. 1227–1230.

Balachandran, B., Zhao, M.X., 1999b. A mechanics-based model for study of dynamics of milling operations. Meccanica, in press.

Davies, M., Balachandran, B., 1999. Impact dynamics in the milling of thin-walled structures. In: Nonlinear Dynamics, in press.

Lin, G.C.I., Oxley, P.L.B., 1972. Mechanics of oblique machining: predicting chip geometry and cutting forces from work material properties and cutting conditions. Proceedings of the Institute of Mechanical Engineering 186, 813–820.

Merritt, H.E., 1965. Theory of self-excited machine-tool chatter. ASME Journal of Engineering for Industry 87, 447–454.

Minis, I., Yanushevsky, R., 1992. A new theoretical approach for the prediction of machine tool chatter in milling. ASME Journal of Engineering for Industry 115, 1–8.

Nayfeh, A., Balachandran, B., 1995. Applied Nonlinear Dynamics: Analytical, Computational, and Experimental Methods. Wiley, New York.

Oxley, P.L.B., 1989. Mechanics of Machining. Wiley, New York.

Sridhar, R., Hohn, R.E., Long, G.W., 1968. A stability algorithm for the general milling process. ASME Journal of Engineering for Industry 90, 330–334.

Tlusty, J., 1985. Machine dynamics. In: King, R.I. (Ed.), Hand Book of High-speed Machining technology. Chapman and Hall, New York, pp. 48–153.

Tlusty, J., Polacek, M., 1963. The stability of the machine tool against self-excited vibration in machining. International Res. Prod. Engng. 465–474.

Tlusty, J., Ismail, F., 1981. Basic non-linearity in machining chatter. Annals of the CIRP 30, 299–304.

Tobias, S.A., Fishwick, W., 1958. The chapter of lathe tools under othogonal cutting conditions. Transactions of the ASME 80, 1079–1088.

Tobias, S.A., 1965. Machine Tool Vibration. Wiley, New York.